PHYSICAL REVIEW LETTERS

Reduced Effective Spin-Orbital Degeneracy and Spin-Orbital Ordering in Paramagnetic Transition-Metal Oxides: Sr_2IrO_4 versus Sr_2RhO_4

Cyril Martins,[1,2] Markus Aichhorn,[3,1] Loïg Vaugier,[1] and Silke Biermann[1,2]

[1]*Centre de Physique Théorique, Ecole Polytechnique, CNRS, 91128 Palaiseau Cedex, France*
[2]*Japan Science and Technology Agency, CREST, Kawaguchi 332-0012, Japan*
[3]*Institute of Theoretical and Computational Physics, TU Graz, Petersgasse 16, Graz, Austria*

We discuss the notions of spin-orbital polarization and ordering in paramagnetic materials, and address their consequences in transition-metal oxides. Extending the combined density functional and dynamical mean field theory scheme to the case of materials with large spin-orbit interactions, we investigate the electronic excitations of the paramagnetic phases of Sr_2IrO_4 and Sr_2RhO_4. We show that the interplay of spin-orbit interactions, structural distortions and Coulomb interactions suppresses spin-orbital fluctuations. As a result, the room temperature phase of Sr_2IrO_4 is a paramagnetic spin-orbitally ordered Mott insulator. In Sr_2RhO_4, the effective spin-orbital degeneracy is reduced, but the material remains metallic, due to both, smaller spin-orbit and smaller Coulomb interactions. The corresponding spectra are in excellent agreement with photoemission data. Finally, we make predictions for the spectra of paramagnetic Sr_2IrO_4.

Probably the most important consequence of relativistic quantum mechanics in solids is the coupling of spin and orbital degrees of freedom. The concept of spin-orbit coupling (SOC) has been known for more than half a century, and its importance in magnetic materials has been recognized early on. Nevertheless, SOC in nonmagnetic materials has only recently become a hot topic in condensed matter physics, in the context of topological insulators [1], within the search for systems for quantum computing applications. Still, the interplay of spin-orbit (SO) interactions with electronic Coulomb interactions in paramagnetic materials remains a largely unexplored field. This is at least partially due to the seemingly mutually exclusive regimes of their acting: SO interactions are strongest in heavy elements, that is in transition-metal compounds with $5d$ (and, to a lesser extent $4d$) electrons. Coulomb interactions, on the other hand, are believed to be most efficient in $3d$ compounds, due to the more localized $3d$ orbitals. It is only recently that this separation has been questioned, e.g., in [2–5].

In this Letter, we present a particularly striking example for the interplay of SOC and Coulomb interactions: in the room-temperature phase of the $5d$ transition-metal oxide (TMO) Sr_2IrO_4 the combined effect of SOC and distortions from the ideal K_2NiF_4-structure is strong enough to suppress the effective degeneracy of the coupled spin-orbital degrees of freedom. Even moderate Coulomb interactions then induce a Mott localized state. The resulting state—despite of being paramagnetic and paraorbital, i.e., in the absence of any magnetic or orbital order—displays a "spin-orbital order" in the sense that the only hole in the t_{2g} manifold occupies a state of well-defined t_{2g}-projected total angular momentum j_{eff}. This notion generalizes the concept of orbital order, well-known in TMOs, to the case

where neither spin nor orbitals are good quantum numbers. We present—entirely from first-principle calculations—a scenario for the paramagnetic insulating state of Sr_2IrO_4, in comparison to the isostructural and isoelectronic $4d$ compound Sr_2RhO_4. For the latter, we find that the smaller SOC and Coulomb interactions induce a partially spin-orbitally polarized metallic state. We calculate photoemission spectra for both materials and find excellent agreement with available experiments.

Sr_2IrO_4 is a $5d$ TMO with a tetragonal crystal structure whose symmetry is lowered from the K_2NiF_4-type, well-known in Sr_2RuO_4 or La_2CuO_4, by $11°$ rotation of its IrO_6 octahedra around the **c**-axis as in its $4d$ counterpart Sr_2RhO_4 [6,7]. Although each Ir site accommodates 5 electrons, Sr_2IrO_4 exhibits an insulating behavior at all temperatures with an optical gap of about 0.26 eV at room temperature [8]. Below 240 K, canted-antiferromagnetic (AF) order sets in, with an effective paramagnetic moment of 0.5 μ_B/Ir and a saturation moment of 0.14 μ_B/Ir [9]. This phase has triggered much experimental and theoretical work recently [3,4,10,11], highlighting, in particular, the importance of the SOC ζ_{SO}. SOC was also shown to be relevant in Sr_2RhO_4, which is a paramagnetic metal down to 36 mK [12]: density functional calculations within the local density approximation (LDA), augmented by Coulomb interactions within the LDA $+ U$ method, reproduce the Fermi surface only if SO interactions are taken into account [13,14].

Here, we focus on the *paramagnetic* insulating phase of Sr_2IrO_4 above 240 K, which has not been addressed by theory before. We analyze the electronic properties by a combination of the LDA with dynamical mean field theory (DMFT). To this effect, we have generalized the LDA + DMFT scheme as implemented in [15] to include SO

interactions [16]. The Coulomb interactions are calculated from the constrained random phase approximation (cRPA) [17], taking matrix elements in the same set of localized orbitals as used in the DMFT calculations [18]. For Sr_2IrO_4 we estimate the Slater integrals as $F^0 = 2.2$ eV and $J = 0.3$ eV, giving an intraorbital Hubbard U in the half-filled $j_{eff} = 1/2$ orbitals of $U = 2.25$ eV [19].

Within an LDA band picture [20], Fig. 1(d), a metallic solution—at variance with experiments—is obtained for Sr_2IrO_4. We construct Wannier functions for the t_{2g} orbitals from the LDA bands within the energy window $[-3.0, 0.5]$ eV. The large SOC of about $\zeta_{SO} \approx 0.4$ eV splits these states into a quartet of states, commonly labeled as $j_{eff} = 3/2$, and a higher lying doublet $j_{eff} = 1/2$. Each state is twice degenerate in $\pm m_j$. The four $j_{eff} = 3/2$ states are almost filled; we find $n_{3/2,|1/2|} = 1.98$ and $n_{3/2,|3/2|} = 1.84$ for the $j_{eff} = 3/2$ orbitals. The $j_{eff} = 1/2$ states thus slightly exceed half-filling with $n_{1/2} = 1.16$. In the left panel of Fig. 2, we plot the j_{eff} character of the Wannier orbitals. The four bands that cross the Fermi level are not purely formed by the $j_{eff} = 1/2$ orbitals, but there is a slight overlap of the $j_{eff} = 1/2$ and $j_{eff} = 3/2 |m_j| = 3/2$ characters, particularly obvious at the Γ point. Similar conclusions were drawn for the AF phase in Ref. [11].

We now redefine the $j_{eff} = 1/2$ and $j_{eff} = 3/2 |m_j| = 1/2$ atomic states, yielding a diagonal density matrix of the local problem. Thus, our definition takes into account the

structural distortions and a tetragonal crystal field in each IrO_6 octahedra. Our coefficients for the $j_{eff} = 1/2$ state are similar to those obtained for the AF phase in Ref. [10].

We now turn to our LDA + DMFT results. In Fig. 3, we display the corresponding spectral functions. Within LDA + DMFT, supplemented by the cRPA interactions, an insulating solution with a Mott gap of the size of the optical gap measured at room temperature (about 0.26 eV [8]) is obtained. Despite the fact that the ARPES measurements of Ref. [3] were performed in the AF phase, a comparison of the total spectral function to the experimental energy distribution curves shows qualitative and even quantitative agreement along the direction Γ-X and Γ-M (between -0.5 eV and -1.5 eV). Along the M-X direction a band around -1 eV is identified. From the orbitally resolved spectral functions [Figs. 3(b) and 3(c)], one can locate the lower $j_{eff} = 1/2$ Hubbard band at about -0.5 eV, in agreement with the ARPES data.

The spin-orbital polarization is enhanced when taking into account Coulomb correlations: the Wannier orbital $j_{eff} = 1/2$ is now exactly half-filled. Moreover, we are now dealing with a state exhibiting (i) a "spin-orbital order" (in the sense of a well-defined j_{eff} quantum number): the upper Hubbard band is of $j_{eff} = 1/2$ type only; (ii) no orbital order: the orbital occupations of the original t_{2g} orbitals to the $j_{eff} = 1/2$ spin orbital are roughly equal, resulting in a vanishing average of the angular momentum operator L_z; (iii) no magnetic order: in contrast to the AF phase, where the $j_{eff} = 1/2$ state also carries the hole, there is no ordering of the corresponding $m_{j_{eff}} = \pm 1/2$ quantum number. We are thus facing the remarkable
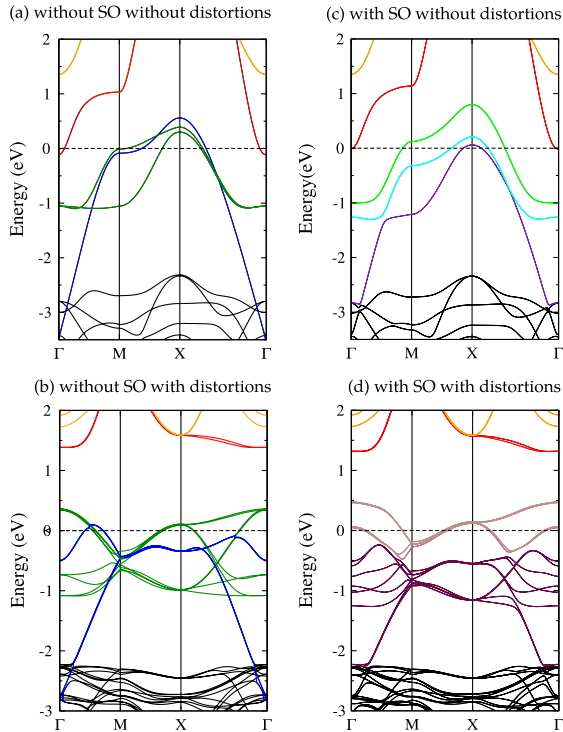

FIG. 1 (color online). LDA band structures of Sr_2IrO_4 without distortions and without SOC (a), with distortions without SOC (b), without distortions with SOC (c) and with both, distortions and SOC (d) [31].
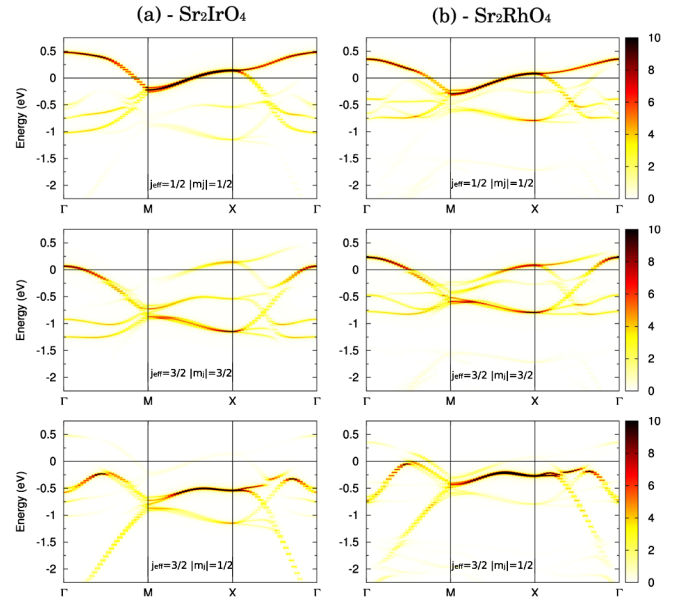

FIG. 2 (color online). LDA band structure of Sr_2IrO_4 (left) and Sr_2RhO_4 (right), projected on the $j_{eff} = 1/2$ (top), $j_{eff} = 3/2$ $|m_j| = 3/2$ (middle), and $j_{eff} = 3/2 |m_j| = 1/2$ (bottom) spin orbitals.

(a) Total spectral density
(b) Spectral density for $j_{eff}=3/2$
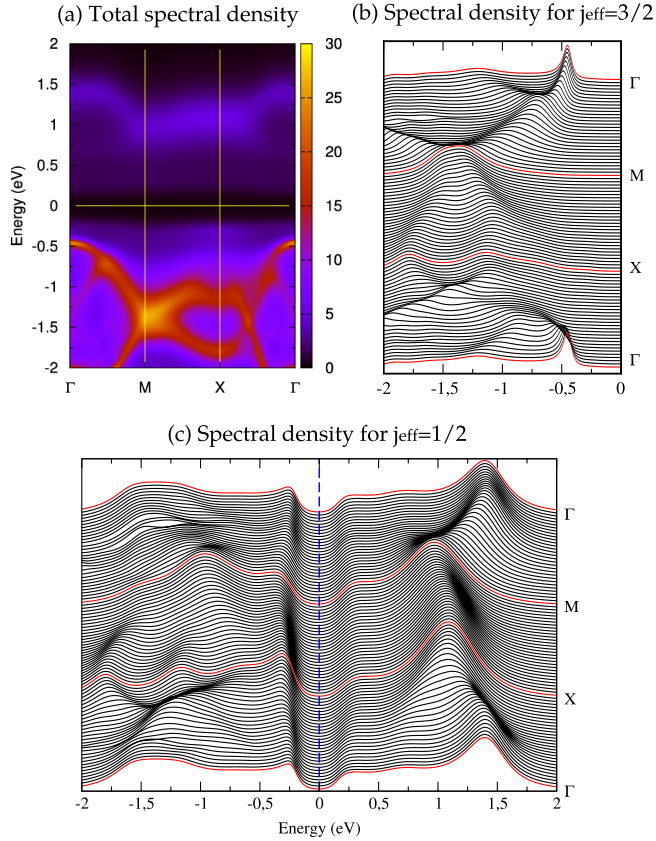(c) Spectral density for $j_{eff}=1/2$

FIG. 3 (color online). Momentum-resolved spectral functions $A(\mathbf{k}, \omega)$ of the paramagnetic phase of Sr_2IrO_4 from LDA + DMFT at $T = 300$ K.

situation of a paramagnetic and paraorbital, but *spin-orbital-ordered* Mott insulator.

As is well known from studies of multiorbital Hubbard models the critical interaction for the formation of the insulating state is lowest for the one-band case, and increases with degeneracy (for a review see [21]). In Sr_2IrO_4, the Hubbard interactions calculated from cRPA are large enough to induce a Mott-insulating state in a half-filled one-orbital but not in a quarter-filled two-orbital or a 1/6-filled three-orbital system. Thus, in Sr_2IrO_4, the reduced effective spin-orbital degeneracy drives the system Mott insulating, even in the paramagnetic state. An analogous suppression of *orbital* degeneracy, albeit purely induced by crystal field splittings, has been studied in the model context in [22,23], and has been found to make $LaTiO_3$ and $YTiO_3$ Mott-insulating [24].

In Sr_2IrO_4, the suppression of *spin-orbital* fluctuations is a consequence of the combined effect of SOC and the tetragonal distortions. To demonstrate this, we do a numerical experiment in which we switch on or off the two effects separately and monitor the critical value of U for the Mott metal-insulator transition.

In Fig. 1(a) both the SOC and the structural distortions are omitted (we use the lattice parameters of Ref. [25]). The band structure of Sr_2IrO_4 is then very similar to the one of Sr_2RuO_4, except for the increased filling compared to the d^4 Ru compound. The t_{2g} orbitals almost equally accommodate the 5 electrons ($n_{d_{xy}} = 1.612$, $n_{d_{xz},d_{yz}} = 1.696$). The insulating Mott state is reached for $F^0 = 3.6$ eV and $J = 0.3$ eV with enhanced orbital polarization. The d_{xy} band gets filled with increasing correlations, approaching a completely filled d_{xy} band and two 3/4-filled $d_{xz/yz}$ bands (which is the atomic ground state). In Fig. 1(b), the SOC is neglected but the structural distortions are included. This lowers the symmetry of Sr_2IrO_4 and results in a four times larger unit cell and four-folded bands. Similarly, as in Sr_2RhO_4 [13], a d_{xy}-$d_{x^2-y^2}$ hybridization gap opens between the e_g and the t_{2g} bands (between 0.4 and 1.3 eV), and the d_{xy} band becomes almost filled. The orbital polarization is thus enhanced compared to the undistorted case, and the Mott transition occurs for smaller values of F^0. Indeed, LDA + DMFT gives the insulating state for $F^0 = 3.0$ eV with $J = 0.3$ eV. In Fig. 1(c), we show the band structure of "undistorted" Sr_2IrO_4 but with SOC. Three j_{eff} bands can be identified: the $j_{eff} = 1/2$ one with an occupation of $n_{1/2} = 1.20$ lies above the two $j_{eff} = 3/2$ ones, with fillings $n_{3/2,|3/2|} = 1.92$ and $n_{3/2,|1/2|} = 1.96$. We find this three band system to be insulating at $F^0 = 3.0$ eV with $J = 0.3$ eV. Although the problem is effectively reduced to an almost half-filled one-band model, the large bandwidth of the $j_{eff} = 1/2$ band prevents a smaller value for the critical F^0. Finally, Fig. 1(d) depicts the band structure of the true compound. In this case, the Mott transition occurs between $F^0 = 2.1$ and 2.2 eV for $J = 0.3$ eV, the values that have been estimated by our cRPA calculations. The combination of both the structural distortions and the SOC is thus necessary for Sr_2IrO_4 to be insulating.

In particular, we would expect Sr_2IrO_4 to be metallic, if either the distortions or the SOC were smaller. Such a situation may be realized if the material is strained, or grown on a substrate [26]. It also occurs in Sr_2RhO_4, the isostructural and isoelectronic 4d counterpart of Sr_2IrO_4. As expected for 4d orbitals, the bandwidth is smaller. As before, we construct Wannier j_{eff} orbitals from the bands within the energy window $[-2.67, 0.37]$ eV; the Wannier j_{eff} character along the bands of Sr_2RhO_4 is shown on the right hand side of Fig. 2. Again, there is a mixture of the $j_{eff} = 1/2$ and $j_{eff} = 3/2$ $|m_j| = 3/2$ orbital character along the four bands crossing the Fermi level. However, since the SOC is weaker in this compound ($\zeta_{SO} = 0.161$ eV) than in its 5d counterpart, the effective splitting between the bands $j_{eff} = 1/2$ and $j_{eff} = 3/2$ $|m_j| = 3/2$ is smaller and these two states have similar filling ($n_{1/2} = 1.42$, $n_{3/2,|3/2|} = 1.64$), whereas the $j_{eff} = 3/2$ $|m_j| = 1/2$ state is filled ($n_{3/2,|1/2|} = 1.96$). The system is thus close to a 3/4-filled two-band model, which favors a metallic state.

Moreover, the Hubbard interactions are smaller than in Sr_2IrO_4: a cRPA calculation as above gives $F^0 = 1.6$ eV and $J = 0.3$ eV for Sr_2RhO_4. Indeed, the weaker
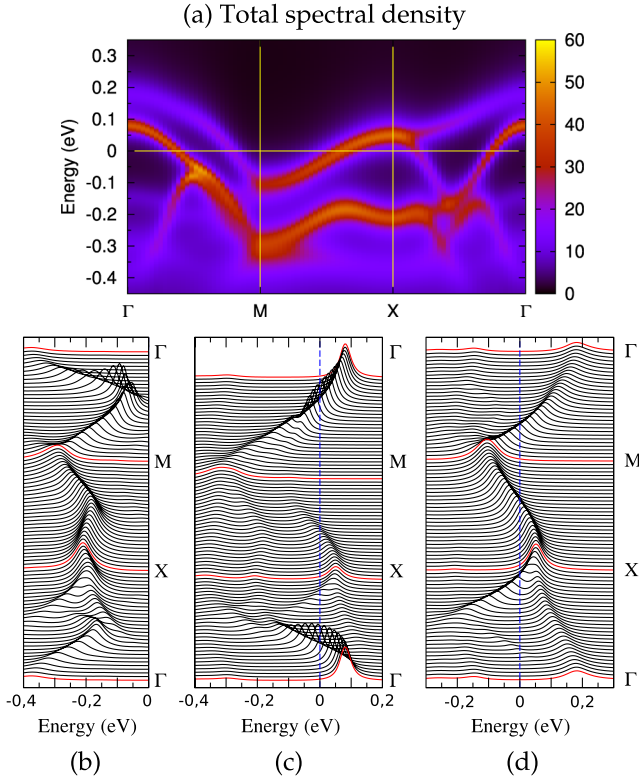
(a) Total spectral density

FIG. 4 (color online).   Momentum-resolved spectral function $A(\mathbf{k}, \omega)$ of Sr_2RhO_4 (a). Bottom panels display the orbitally resolved spectral densities for $j_{eff} = 3/2 \, |m_j| = 1/2$ (b), $j_{eff} = 3/2 \, |m_j| = 3/2$ (c) and $j_{eff} = 1/2$ (d) at $T = 300$ K.

hybridization of the Rh-$4d$ states with the O-$2p$ locates the latter about 1 eV higher in energy than in Sr_2IrO_4. As a result, the Coulomb interactions are screened more efficiently in Sr_2RhO_4 compared to Sr_2IrO_4. By computing the interaction within cRPA for an artificial Sr_2RhO_4 system in which we shift the O-p-states down by 1 eV we verify that F^0 is indeed increased.

Our LDA + DMFT calculations, Fig. 4, are in good agreement with energy distribution curves obtained by ARPES at 10 K [27,28]. We observe a large electronlike pocket of radius 0.65–0.69 Å^{-1} and a smaller hole pocket of radius 0.19–0.18 Å^{-1} in the undistorted Brillouin zone. Further structures are found between -0.1 and -0.2 eV along Γ-X and around -0.1 eV along Γ-M. The orbitally resolved spectral functions allow to attribute both of these structures to the $j_{eff} = 3/2 \, |m_j| = 1/2$ orbital, whereas the holelike α pocket around Γ is of $j_{eff} = 3/2 \, |m_j| = 3/2$ type. The two other pockets, β_M and β_X, are (mostly) of type $j_{eff} = 1/2$.

We find that Sr_2RhO_4 is close to the Mott transition (which would occur for interaction strengths of $F^0 = 1.8$–2.0 eV while keeping J fixed). The occupancies of the $j_{eff} = 1/2$ and $j_{eff} = 3/2 \, |m_j| = 3/2$ spin orbitals are 0.63 and 0.89, respectively. The quasiparticle weights

for $j_{eff} = 1/2$ and $j_{eff} = 3/2$, $|m_j| = 3/2$ have been estimated as $Z_{1/2} = 0.5$ and $Z_{3/2,|3/2|} = 0.6$.

In conclusion, we have shown that only the cooperative effect of SOC, lattice distortions and Coulomb correlations drives the $5d$ compound Sr_2IrO_4 insulating, due to a complete spin-orbital polarization resulting in an effective half-filled one-orbital (more precisely, two-spin-orbital) system. The picture for the high-temperature phase of Sr_2IrO_4 that emerges from our first principles calculations is that of a paramagnetic and paraorbital, but spin-orbital-ordered Mott insulator. The isostructural and isoelectronic $4d$ compound Sr_2RhO_4 has smaller SOC and Coulomb interactions, leading to a less dramatic reduction of spin-orbital fluctuations and, as a result, a two-orbital (or four spin-orbital) metal. The structural and electronic similarities between Sr_2IrO_4 and La_2CuO_4 [29]—both are Mott insulators with one hole in an effective one-orbital system—together with the pronounced difference in their magnetic structure, suggest that the transport properties of *doped* Sr_2IrO_4 may give valuable information about the role of magnetic fluctuations in high-T_c superconductivity. Oxygen-deficient Sr_2IrO_4 is not superconducting [30]. Our electronic structure calculations show, however, that doping by impurities with extremely weak SOC should act as giant perturbations to the spin-orbital structure, in analogy to introducing a *magnetic* impurity into a system with weak SOC. It would be most interesting to introduce carriers into the system while conserving as much as possible the very specific electronic structure, e.g., by doping with heavy atoms such as Os or Re.

[1] C. L. Kane and E. J. Mele, Phys. Rev. Lett. **95**, 146802 (2005).
[2] S. J. Moon et al., Phys. Rev. Lett. **101**, 226402 (2008).
[3] B. J. Kim et al., Phys. Rev. Lett. **101**, 076402 (2008).
[4] B. J. Kim et al., Science **323**, 1329 (2009).
[5] D. Pesin and L. Balents, Nature Phys. **6**, 376 (2010).
[6] Q. Huang et al., J. Solid State Chem. **112**, 355 (1994).
[7] M. Itoh et al., J. Solid State Chem. **118**, 206 (1995).
[8] S. J. Moon et al., Phys. Rev. B **80**, 195110 (2009).
[9] G. Cao et al., Phys. Rev. B **57**, R11 039 (1998).
[10] H. Jin et al., Phys. Rev. B **80**, 075112 (2009).
[11] H. Watanabe, T. Shirakawa, and S. Yunoki, Phys. Rev. Lett. **105**, 216410 (2010).
[12] S. J. Moon et al., Phys. Rev. B **74**, 113104 (2006).
[13] M. W. Haverkort et al., Phys. Rev. Lett. **101**, 026406 (2008).
[14] G.-Q. Liu et al., Phys. Rev. Lett. **101**, 026408 (2008).
[15] M. Aichhorn et al., Phys. Rev. B **80**, 085101 (2009).

[16] C. Martins, M. Aichhorn, and S. Biermann (to be published).

[17] F. Aryasetiawan *et al.*, Phys. Rev. B **70**, 195104 (2004).

[18] L. Vaugier, H. Jiang, and S. Biermann (to be published).

[19] Note, however, that for computational reasons these parameters were calculated for the undistorted phases without SOC. Screening with e_g states is excluded in the range of the hybridization gap in order to mimic the band structure of the distorted material. We then transform to the basis of t_{2g}-projected total angular momentum eigenstates, keeping density-density interaction terms only.

[20] P. Blaha *et al.*, *Wien2k, An Augmented Plane Wave + Local Orbitals Program for Calculating Crystal Properties* (Karlheinz Schwarz, Tech. Universität Wien, Austria, 2001).

[21] A. Georges, S. Florens, and T. A. Costi, J. Phys. IV (Colloque) **114**, 165 (2004).

[22] N. Manini *et al.*, Phys. Rev. B **66**, 115107 (2002).

[23] A. I. Poteryaev *et al.*, Phys. Rev. B **78**, 045115 (2008).

[24] E. Pavarini *et al.*, Phys. Rev. Lett. **92**, 176403 (2004).

[25] J. J. Randall, L. Katz, and R. Ward, J. Am. Chem. Soc. **79**, 266 (1957).

[26] Because of the similarity of the lattice constant of $SrTiO_3$, Sr_2IrO_4 on $SrTiO_3$, e.g., should be nearly undistorted.

[27] F. Baumberger *et al.*, Phys. Rev. Lett. **96**, 246402 (2006).

[28] R. S. Perry *et al.*, New J. Phys. **8**, 175 (2006).

[29] F. Wang and T. Senthil, Phys. Rev. Lett. **106**, 136402 (2011).

[30] O. B. Korneta *et al.*, Phys. Rev. B **82**, 115117 (2010).

[31] Bands in color (online) are the Ir-$5d$ bands, each color corresponding to a different character.